ELSEVIER

Contents lists available at ScienceDirect

Micro and Nano Engineering

journal homepage: www.sciencedirect.com/journal/micro-and-nano-engineering



Evaluation of industrial and consumer 3-D resin printer fabrication of microdevices for quality management of genetic resources in aquatic species

Seyedmajid Hosseini ^a, Jack C. Koch ^{b,*}, Yue Liu ^b, Ignatius Semmes ^c, Isabelina Nahmens ^d, W. Todd Monroe ^c, Jian Xu ^a, Terrence R. Tiersch ^{b,*}

- ^a Department of Electrical & Computer Engineering, Louisiana State University, Baton Rouge, LA, USA
- b Aquatic Germplasm and Genetic Resources Center, School of Renewable Natural Resources, Louisiana State University Agricultural Center, Baton Rouge, LA, USA
- c Department of Biological & Agricultural Engineering, Louisiana State University and Louisiana State University Agricultural Center, Baton Rouge, LA, USA
- ^d Department of Mechanical & Industrial Engineering, Louisiana State University, Baton Rouge, LA, USA

ARTICLE INFO

Keywords: Germplasm repository Aquatic species 3-D resin printing Soft lithography Photolithography Aquaculture industry Genetic resources

ABSTRACT

Aquatic germplasm repositories can play a pivotal role in securing the genetic diversity of natural populations and agriculturally important aquatic species. However, existing technologies for repository development and operation face challenges in terms of accuracy, precision, efficiency, and cost-effectiveness, especially for microdevices used in gamete quality evaluation. Quality management is critical throughout genetic resource protection processes from sample collection to final usage. In this study, we examined the potential of using three-dimensional (3-D) stereolithography resin printing to address these challenges and evaluated the overall capabilities and limitations of a representative industrial 3-D resin printer with a price of US\$18,000, a consumer-level printer with a price <US\$700, and soft lithography, a conventional microfabrication method. A standardized test object, the Integrated Geometry Sampler (IGS), and a device with application in repository quality management, the Single-piece Sperm Counting Chamber (SSCC), were printed to determine capabilities and evaluate differences in targeted versus printed depths and heights. The IGS design had an array of negative and positive features with dimensions ranging from 1 mm to 0.02 mm in width and depth. The SSCC consisted of grid and wall features to facilitate cell counting. The SSCC was evaluated with polydimethylsiloxane (PDMS) devices cast from a typical photoresist and silicon mold. Fabrication quality was evaluated by optical profilometry for parameters such as dimensional accuracy, precision, and visual morphology. Fabrication time and cost were also evaluated. The precision, reliability, and surface quality of industrial-grade 3-D resin printing were satisfactory for operations requiring depths or heights larger than 0.1 mm due to a low discrepancy between targeted and measured dimensions across a range of 1 mm to 0.1 mm. Meanwhile, consumer-grade printers were suitable for microdevices with depths or heights larger than 0.2 mm. While the performance of either of these printers could be further optimized, their current capabilities, broad availability, low cost of operation, high throughput, and simplicity offer great promise for rapid development and widespread use of standardized microdevices for numerous applications, including gamete quality evaluation and "laboratory-on-a-chip" applications in support of aquatic germplasm repositories.

1. Introduction

Throughout history, ensuring the protection of economically important agricultural species has involved the storage, assessment, and distribution of genetic resources. One preservation method for these resources involves placing them in a frozen state, a technique known as

cryopreservation. Cryopreserved samples are commonly stored in collections or repositories [1–4]. However, scalable cryopreservation technologies and germplasm repositories are not in place for most aquatic species despite the urgent need to protect the genetic resources that provide the foundation for aquaculture, food security, biomedical research, conservation, and wild fisheries. The genetic resources that

E-mail addresses: jkoch@agcenter.lsu.edu (J.C. Koch), ttiersch@agcenter.lsu.edu (T.R. Tiersch).

https://doi.org/10.1016/j.mne.2024.100277

Received 15 June 2024; Received in revised form 15 July 2024; Accepted 23 July 2024 Available online 25 July 2024

2590-0072/© 2024 The Authors. Published by Elsevier B.V. This is an open access article under the CC BY-NC license (http://creativecommons.org/licenses/by-nc/4.0/).

^{*} Corresponding authors.

support billions of dollars [5] of capture fisheries and human livelihoods are not protected, and the risk and expense of maintaining live animals (rather than frozen samples) hinder the growth of numerous aquatic industries [6]. These risks and expenses can be minimized by developing proprietary or shared (open) hardware devices that are capable of accelerating repository development and aiding in management and processing operations for the protection of genetic resources [7].

The growing climate crisis has exacerbated costs, risks, and needs associated with safeguarding genetic resources of aquatic species around the world. A vast majority of aquatic species that are important for aquaculture, food security, biomedical research, conservation, and wild fisheries are native to low-to-middle income nations where genetic resource protection is not a long-term priority or where equipment and reliable resources are scarce. Policy and long-term agendas must be addressed at scales beyond the individual. With the rapid growth of open-additive manufacturing, sustainable capabilities and resources can become widely accessible, and can be developed, customized, and fabricated by anyone.

Reliable tools and devices are essential for safeguarding genetic resources because they enable critical processing and quality management (QM) steps from sample collection to final usage. A relevant example is Bangladesh which is home to >600 species of freshwater and marine fishes. These fishes provide a primary protein source to sustain a growing human population of 171 million. Land use changes, introduced species, overharvesting, and other anthropogenic effects have strained open-water fisheries, and the country now relies heavily on farmed fishes (i.e., aquaculture) [8] with a narrowing gene pool. Cryopreservation is essential for preserving quality genetics, sustaining livlihoods, and ensuring sustainable production and improvement of aquatic species in Bangladesh and abroad. There are ongoing efforts to develop germplasm repositories for aquatic species in Bangladesh [8,9], but access to reliable tools and supplies, especially for quality management, are major roadblocks to these efforts. These same urgent needs for protection of aquatic genetic resources exist throughout the world, including the United States.

Capability needs for cryopreservation are driven by processing steps such as germplasm collection (e.g., sperm, eggs, early life stages, cells), quality evaluation, cryopreservation, storage, thawing, and final usage. Sample quality is of critical importance as the samples frozen today may be stored for decades and processing of poor quality samples wastes time and resources today and in the future. Quality management is a major driving force behind the need to develop novel, customizable, and accessible microdevices (e.g., micromixers [10], microfluidic lab-on-achip systems [11], and micro-separators [12]) to assist in safeguarding aquatic genetic resources. Such microdevices need to be versatile and practical for activities centered around germplasm QM, including quality planning, quality assurance (QA, process oriented), quality control (QC, product oriented), quality evaluation, and quality improvement.

There are existing devices to accomplish these processes, but they are often fixed in design, not suitable for multiple species, and prohibitively expensive for global deployment. For example, the process of counting sperm to calculate concentration can be accomplished by use of commercial devices such as a hemocytometer (>US\$100) or a Makler chamber (>US\$750) with counting by eye (which requires experience and is prone to variation) or by use of a computer-assisted sperm analysis (CASA) system (highly repeatable but >US\$25,000). Integration of open-hardware microfluidic and microdevice systems would play a pivotal role in ensuring the dependable quality of germplasm materials, facilitating the isolation and culture of gametes and embryos, and optimizing the efficiency of sperm sorting and separation [13].

The use of soft lithography to develop microdevice systems (e.g., the Microfabricated Enumeration Grid Chamber [MEGC, 14] or the Single-piece Sperm Counting Chamber [SSCC, 15]) began to address some of the issues with sperm counting devices but suffer from prohibitively expensive initial costs and a lack of efficient options for iterative

customization. Soft lithography typically makes use of the material, polydimethylsiloxane (PDMS) which yields high-resolution parts with excellent surface finish and low cytotoxicity [14-18]. In traditional PDMS-based soft lithography, microdevice fabrication relies on a master mold created through intensive soft lithography processes (e.g., photolithography and etching) [19]. Microdevice creation entails pouring the PDMS onto the master mold, letting it cure, and peeling it off to replicate the mold pattern. Despite its effectiveness, this process is expensive, time-consuming, complex [20], and has a number of drawbacks that limit use, especially for rapid prototyping. Soft lithography is more than capable of fabricating high-resolution devices for germplasm samples that exist at the smallest size ranges of aquatic germplasm (e.g., sperm of zebrafish [0.002 mm head width] or swordtails [0.001 mm head width]). However, it is not reliable for creating devices with larger or varied heights and depths that are required for most other species, and is slow, costly, and restricted to specialized facilities. In this study, we did not directly compare PDMS and resin prints, although such evaluations have been conducted in the past [21-26]. Instead, our focus was on the evaluation of the potential for shifting to new fabrication techniques, including overall consideration of factors such as cost reduction. improved fabrication accessibility, and development of open-hardware communities based on the sharing of digital design files.

Three-dimensional (3-D) resin printing techniques such as stereolithography (SLA) and digital light projection (DLP) offer a promising and effective alternative to soft lithography and are gaining traction in the development and prototyping of microdevices. These rapidly advancing technologies can play a crucial role in addressing the creation of hardware devices with broad applications in genetic resource protection [14,15,27,28]. Three-dimensional resin printers surpass many of the constraints of soft lithography and other traditional methods through layer-by-layer transformation of computer-aided designs into tangible hardware, crafting accurate 3-D shapes. This process eliminates the need for photo masks, alignment processes, etching, and bonding which require specialized facilities and well-trained personnel, offering a more efficient and flexible manufacturing approach [29]. In addition, resin printers have access to thousands of resin types, including those developed for application in human medicine (e.g., dental-grade resins) and for use with germplasm [e.g., [30]].

Two major levels of resin printers are industrial-grade and consumergrade. In general, consumer-grade printers have lower prices (US\$400 – US\$1,000) and lower-grade components, often limiting the resolution that can be achieved. Industrial-grade printers come with greater upfront costs (>US\$10,000) but have higher-grade components, access to customizable resin materials, optimized resin polymerization, and system processing features for faster and more successful prints. Even the higher-priced machines, however, are much more widely available and less expensive than traditional soft lithography. Although some groups have taken the approach of pushing the capabilities of consumergrade printers, a slow and resource-intensive process [31], there are few studies that evaluate the accuracy and precision available and resources required for device fabrication using these different techniques (resin printing and soft lithography) and printer types (industrial and consumer). This understanding is vital for aquaculture and aquatic research communities outside of traditional engineering departments. Consumergrade products are beneficial because of their accessibility, but for technology developers, it may be more advantageous to prototype quickly with industrial-grade printers before pushing the boundaries of consumer-grade products to make devices widely available. By finding a balance among these factors, 3-D resin printing can offer new opportunities for rapid prototyping and production of micro-scale devices as an alternative to conventional soft lithographic methods.

Thus, the goal of this study was to evaluate the capabilities of 3-D resin printers and demonstrate the fabrication quality of microdevices using industrial and consumer 3-D resin printers and conventional soft lithography (photolithography) techniques. The specific objectives were to: 1) evaluate accuracy and precision in feature fabrication with opaque

and clear resins; 2) assess the accuracy and precision between fabrication techniques (resin printing and photolithography), particularly for small features (<1 mm); 3) analyze the visual morphology of features produced by different methods, and 4) evaluate the utility, time, and cost requirements for overall comparison of microfabrication among the methods.

2. Materials and methods

2.1. Device description and fabrication

There is a wide range of forms and functions of microdevices. This study evaluated two representative devices: one with real-world application and one specifically designed to test the limits of resin 3-D printers. Both devices were designed using computer-aided design (CAD) software (Fusion 360, Autodesk, San Rafael, CA, USA) for systematic evaluations. The first was the Single-piece Sperm Counting Chamber (SSCC) [15], which consisted of grid and wall features with height of 0.01 mm (photolithography) or 0.1 mm (resin printing), including gaps in the gridlines that connect the squares to allow better distribution of samples for counting or quality evaluation (e.g., sperm motility) (Fig. 1, left column images). This difference in wall height between fabrication technologies prevented direct comparison but was necessary based on the current limitations and nature of the technological processes (e.g., photolithography spinning and resin printing layer height). The SSCC was specifically designed to accurately count sperm concentration in aquatic species such as zebrafish [15]. Its functionality heavily depends on the chamber volume, ensuring precise counting. This chamber provides a simple, customizable, and costeffective alternative to traditional counting methods, aiding research in reproductive biology and assisted reproduction technologies.

The second was the Integrated Geometry Sampler (IGS), which featured an array of negative and positive features such as a semi-spheres, channels with dimensions ranging from 1 mm to 0.02 mm in width and depth, and concentric circles ranging in diameter from 4.2 mm to 0.6 mm and with step sizes of 0.2 mm (Fig. 1, right column images). Fabricating the IGS with traditional photolithography techniques would be cumbersome due to the many different feature heights on the device, each of which necessitates a separate masking, exposure, and development process. The IGS was designed specifically to evaluate the fabrication quality of 3-D resin printers.

2.1.1. Fabrication by use of soft lithography

The photolithography-based SSCC devices evaluated in this study were fabricated using a master mold created previously [12] on a silicon

wafer. The process is briefly described below. A clean silicon wafer (UniversityWafer Inc., South Boston, MA, USA) served as a mold substrate. A 0.01-mm layer of SU-8 photoresist (MicroChem Corp., Newton, MA, USA) was spin-coated (Laurell Technologies Corporation, North Wales, PA, USA) on the wafer. This photoresist was chosen for its resolution and ease of microfabrication [32]. Spin-coater settings (e.g., rotational velocity) and photoresist type [33] determine the minimum and maximum feature height that can be achieved. A precisely aligned mask was set on top of the wafer to transfer the pattern during UV light exposure (American Ultraviolet®, Lebanon, IN, USA). The unexposed SU-8 photoresist was subsequently removed by application of SU-8 developer (MicroChem Corp., Newton, MA, USA), revealing the pattern on the wafer. A 10:1 mixture of PDMS and curing agent (Sylgard-184, Sigma-Aldrich, Inc., MO, USA) was prepared according to the manufacturer's specifications and was poured onto the mold, covering the SSCC pattern. To remove air bubbles, the PDMS was degassed in a vacuum chamber, followed by curing in an oven at 70 °C for 2 h to solidify the PDMS. The de-molded PDMS was cleaned with 70% isopropyl alcohol (IPA), deionized (DI) water, and dried with nitrogen gas.

2.1.2. Selection of 3-D printers and resin materials

This study evaluated two 3-D resin printer models representative of current (as of January 2024) industrial and consumer levels. This work was not intended as a direct comparison of manufacturers or models. To broadly evaluate the capabilities of 3-D resin printers and microfabrication, we chose an industrial 3-D resin printer (Profluidics 285D, CADworks3D, Concord, ON) and a consumer-grade printer (Sonic Mighty 8K, Phrozen, Hsinchu City, Taiwan). The IGS produced using the industrial 3-D printer was evaluated against another made with the consumer 3-D printers were also evaluated with a photolithography-based SSCC, although this was again not intended to be a direct comparison because of a pre-selected difference in the SSCC grid-wall heights (0.1 mm for resin printers and 0.01 mm for photolithography).

The industrial 3-D printer had a 28.5-µm dynamic pixel size and an approximate cost of US\$18,000. For the fabrication of devices with the industrial 3-D printer, opaque green mastermold resin (CADworks3D, Concord, Ontario) and clear microfluidic resin (CADworks3D) were used. The consumer 3-D resin printer had a 28-µm pixel size and cost approximately US\$700. For fabrication of devices with the consumer 3-D printer, opaque gray Aqua 8K resin (Phrozen, Hsinchu City, Taiwan) and Nova3D ultra-clear resin (Nova3D, Guangdong, China) were used.

2.1.3. Three-dimensional resin printing process **Pre-processing:**

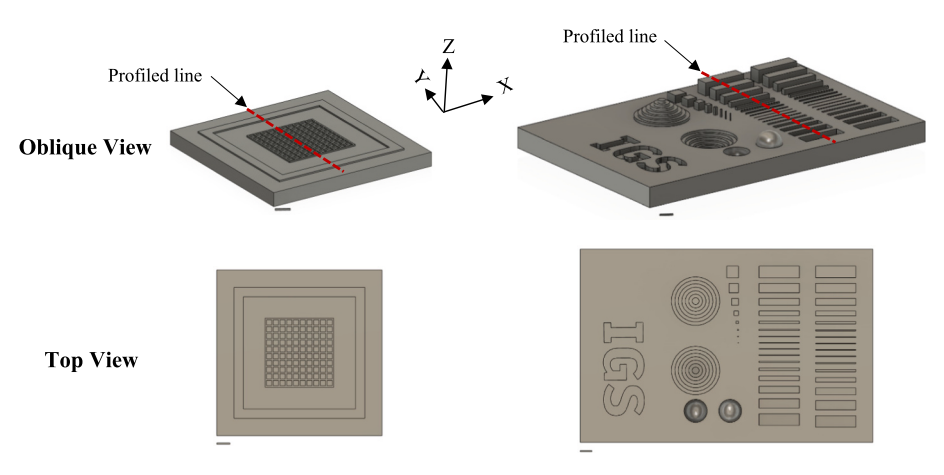


Fig. 1. Three-dimensional schematics illustrating the Single-piece Sperm Counting Chamber (SSCC) (oblique and top views, left column), and the Integrated Geometry Sampler (IGS) (oblique and top views, right). Scale bars are 1 mm. Dotted red lines represent the profile transects (X, Y, and Z) evaluated by profilometry. (For interpretation of the references to colour in this figure legend, the reader is referred to the web version of this article.)

During the printer slicing process for the SSCC and IGS models, variations were introduced to the dimensions because the slicer needed to adjust the lateral measurements to align with the pixel sizes (\sim 28 μ m) of the LCD array - i.e., the printer cannot use half a pixel to accommodate a specific dimension [34]. This device-pixel alignment improved grid line consistency and uniformity in square designs. Thus, the X-Y dimensions of each device were scaled by a factor of 28. For example, the SSCC width was set at 392 µm, which is divisible by 28. Designs were converted to STL format for slicing using Utility (Ver 6.4.4.t12) for the industrial 3-D printer and LycheeSlicer (Ver 5.2.201) for the consumer 3-D printer. Multiple printing configurations were evaluated for both printers and the chosen settings are listed in Supplementary Table 1. These settings were selected to balance printing of positive and negative features. Based on printer behavior with specific geometries (e.g., a channel printed 20% deeper than expected), device dimensions (e.g., decreased channel depth) and slicer settings can be optimized to target positive or negative features. This study thus evaluated print quality without focus on single fine-tuned adjustments, illustrating the mechanical precision and accuracy differences of industrial and consumergrade resin printers across a composite range of feature types and sizes that would occur in quality-management devices for aquatic species.

Post-processing:

After printing, residual resin was removed by immersing the devices in a plastic bag containing 70% IPA and placing the bag into an ultrasonic water bath for 4 min. The devices were rinsed with fresh 70% IPA and DI water to ensure the complete removal of uncured resins. After 2 min of air drying, devices were exposed to a 405 nm UV light (Elegoo, Mercury X Cure, China) for 1 min to complete curing and post-processing.

2.2. Fabrication quality assessment

Comparison of multiple device features was used to provide insight into fabrication quality, accuracy, and precision among the different fabrication technologies and served as a preliminary evaluation for the widespread transition from conventional microfabrication approaches to 3-D resin printing. In fabrication of microdevices such as microchannels, clarity in the final device is crucial for use in light microscopy. While clear resin is typically preferred for this purpose in 3-D resin printing, we encountered challenges from reflected light when conducting profilometry on devices crafted from clear resin, which hampered dimensional measurements. To address this, we conducted experiments wherein devices were fabricated in parallel using opaque and clear resins.

To directly address the profiling of clear resin, a thin coating (<0.005 mm) of titanium dioxide (TiO₂) nanoparticles was applied to devices. Titanium dioxide nanoparticles were suspended in isopropanol (0.1 mg/ml) and spray coated by use of an airbrush to enhance the surface optical properties (Semmes et al., unpublished data). The gray devices did not require the addition of a TiO₂ coating layer. All devices were scanned by use of an optical profiler (Keyence VR-6100, Osaka, Japan) that used non-destructive, non-contact analysis principles. The profiler utilized light to examine surface topography, splitting the light source into two paths: one directed at the surface and the other at a reference mirror. Upon recombination, reflections were projected onto an array detector, enabling precise (0.001 mm) measurements with minimal interference. Dimensional measurements were analyzed using 3D Optical Profilometer VR-6000 software (Keyence). The reference plane for the SSCC was at the bottom of the counting chamber, and for the IGS was at the middle surface between negative and positive features.

While simple 3-D printed parts with large feature sizes can be assessed by visual observation for suitability, microdevices with features and dimensions that differ from the target dimensions (e.g., micromixers) can show altered performance and require closer inspection upon fabrication. Thus, this study evaluated accuracy and precision of

printed device features. Accuracy refers to the closeness of measured values to target values, while precision indicates the consistency and reproducibility of measurements. These metrics are crucial for understanding the reliability and performance of fabrication processes, particularly in the context of transitioning from conventional microfabrication methods to emerging 3-D printing techniques. In this study, accuracy was evaluated by the difference between the target dimension and the mean of measured dimensions (photolithography, n=6 measurements on 1 device; resin printing, n=6 measurements each on 4 devices). Precision was assessed by calculating the standard deviation to quantify consistency and reproducibility of the fabrication processes.

To visually assess surface morphology and examine small changes in residual resin, samples were examined by use of a scanning electron microscope (SEM) (JSM -6610 LV SEM, Jeol USA, Peabody, MA, USA). Preparing devices for SEM imaging involved several steps to achieve high-resolution images. Devices were cleaned with IPA, rinsed with DI water, and air dried. A thin layer of titanium was sputter-coated onto the sample to prevent charging and improve image quality. Prepared devices were loaded into the SEM chamber. A high vacuum was pulled on the chamber in preparation for imaging. Devices were positioned and images from several angles and magnifications were captured for later visual analyses.

2.3. Time and cost requirements of microfabrication techniques

An evaluation was conducted of the time and cost associated with fabrication, assessing photolithography-based SSCC and devices printed by use of 3-D resin printing. For the photolithography time estimate, we assumed that all necessary equipment was at one facility to perform typical tasks as follows: mask preparation, spin-coating SU-8 photoresist, aligning and UV exposing, developing and curing the photoresist, pouring the PDMS mixture onto the mold, vacuum degassing, curing in an oven, and cleaning and drying the de-molded PDMS. For evaluation, the total printing duration comprised the active printing time (provided by the 3-D printer) and the associated pre-processing (e.g., slicing) and post-processing (e.g., cleaning and curing) steps. For photolithography, costs included mask creation, silicon wafer production, SU-8, SU-8 developer, and PDMS; for the 3-D printers, the cost calculation incorporated the expenses of resin materials.

3. Results

3.1. Accuracy and precision in feature fabrication with opaque resin

Dimensional accuracy (difference between target dimensions and the mean of measured dimensions) and precision (standard deviation) were assessed in fabrication of negative features (microchannel depth) on the IGS using opaque resins. For channel depths of 0.4–1 mm, the industrial 3-D printer depth showed a difference of <2% between the target and measured dimensions (Fig. 2a). In contrast, the consumer 3-D printer displayed a 3–8% discrepancy in channel depths across this range. For smaller channels of 0.1–0.2 mm, the industrial 3-D printer depth showed a difference of about 13% (Fig. 2b). Using the settings described herein, the consumer printer failed to reliably fabricate channels <0.2 mm. The standard deviation of measurements for all channel depths ranged from 0.011 to 0.039 mm for the industrial 3-D printer configuration. In comparison, the consumer printer exhibited standard deviation values ranging from 0.018 to 0.046 mm for all channel depths.

Analysis of the accuracy of positive features (raised microchannels) on the IGS using opaque resins for heights of 0.4–1 mm fabricated by the industrial 3-D printer showed a difference of <2% between the target and measured dimensions (Fig. 2a). In contrast, evaluation of the accuracy of positive (raised) features produced by the consumer 3-D printer revealed fluctuations exceeding 30%. For smaller heights of 0.1–0.2 mm, the industrial 3-D printer depth showed a difference of about 19% (Fig. 2b). The standard deviation of measurements for all

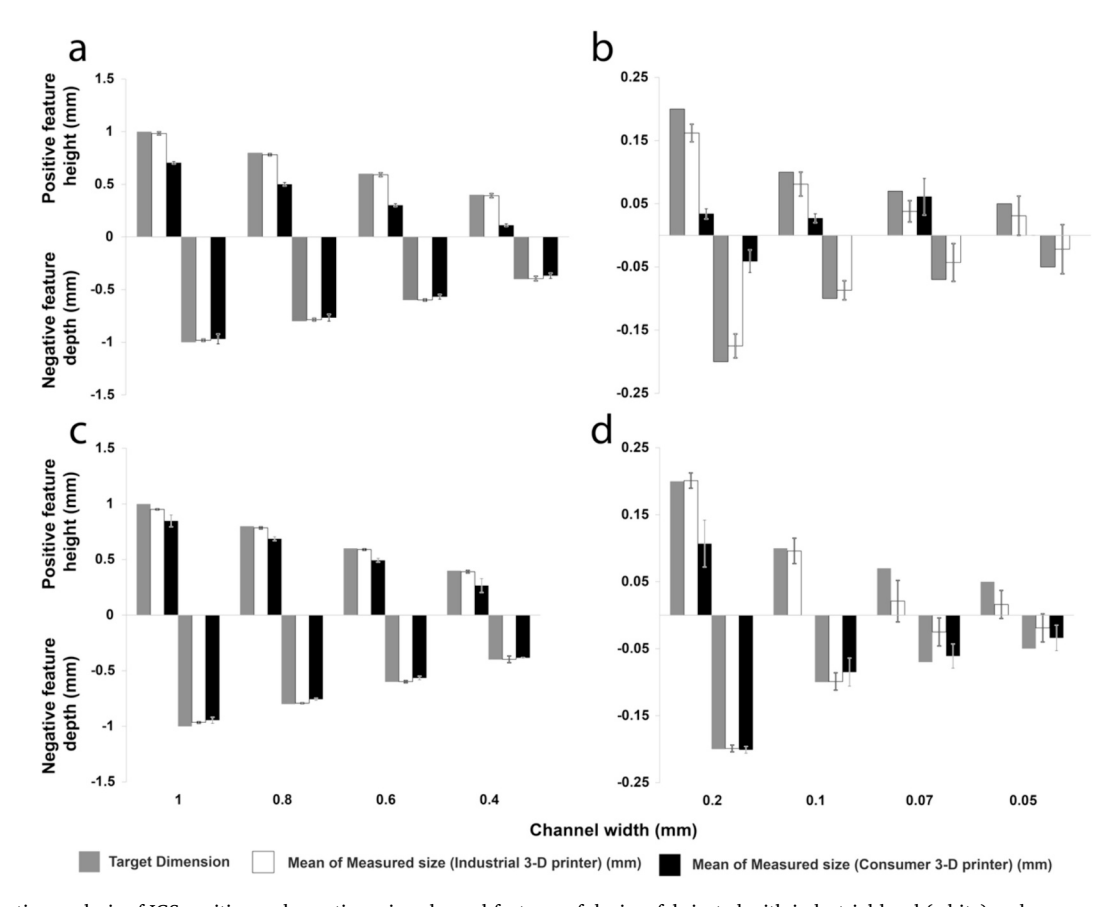


Fig. 2. Comparative analysis of IGS positive and negative microchannel features of devices fabricated with industrial-level (white) and consumer-level (black) 3-D resin printers compared to target dimensions (gray). Devices were printed using opaque resin with features ranging from 1 to 0.4 mm (panel a), and ranging from 0.2 to 0.05 mm (b); and clear resin with features ranging from 1 to 0.4 mm (c), and ranging from 0.2 to 0.05 mm (d). Sample size of four devices with six measurements per device were averaged and error bars were reported as standard deviation.

channel heights ranged from 0.01 to 0.031 mm for the industrial 3-D printer. In comparison, the consumer 3-D printer exhibited standard deviation values ranging from 0.007 to 0.029 mm.

Seven positive and seven negative stepped features were designed in the IGS with heights and depths of $0.2\,\mathrm{mm}$ per step ($1.4\,\mathrm{mm}$ overall). For the first five negative stepped features the depths fabricated with the

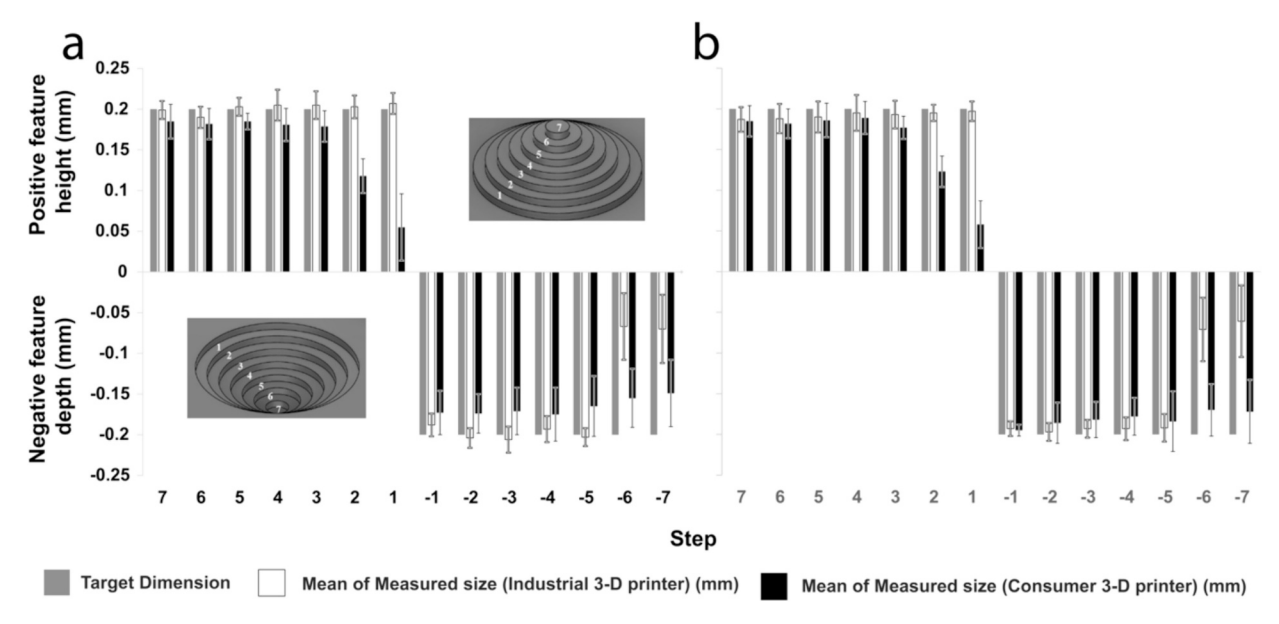


Fig. 3. Comparative analysis of IGS stepped features (negative and positive) fabricated with industrial (white) and consumer-level (black) 3-D resin printers compared to target dimensions (gray). The devices were printed with seven positive and seven negative stepped features using opaque resin (panel a), and clear resin (b). Four devices with six measurements per device were averaged and error bars were reported as standard deviation.

industrial 3-D printer showed a difference of <6% between the target and measured dimensions (Fig. 3a). In contrast, the consumer-level printer displayed a 12–26% discrepancy between target and measured dimensions in seven-stepped feature depths. Using the settings described herein, the industrial printer failed for the last two bottom (6th and 7th) stepped features. The standard deviation of depth measurement ranged from 0.011 to 0.042 mm for the industrial printer. In comparison, the consumer printer exhibited standard deviation values ranging from 0.024 to 0.041 mm.

For the positive stepped features (diameter range from $4.2~\mathrm{mm}$ to $0.6~\mathrm{mm}$), accuracy of the industrial 3-D printer had a difference of <5% between the target and measured heights. In contrast, accuracy of positive stepped features produced by the consumer printer was <11% other than the first and second round features (diameters of $4.2~\mathrm{and}~3.6~\mathrm{mm}$) which deviated from the target values by over 40%. The standard deviation of height measurement ranged from 0.011 to $0.019~\mathrm{mm}$ for the industrial printer. In comparison, the consumer printer exhibited standard deviation values ranging from 0.01 to $0.041~\mathrm{mm}$ (Fig. 3a).

Analysis of the accuracy of the opaque SSCC (with a grid height of 0.1 mm) fabricated with the industrial 3-D printer had a 4% discrepancy between target and measured heights (Fig. 4). The consumer printer had a discrepancy of 37% in dimensional height when utilizing opaque resin. The standard deviation for the samples fabricated with the industrial printer was 0.003 mm. Despite the discrepancies with the consumer printer, the standard deviation was 0.004 mm.

3.2. Accuracy and precision in feature fabrication with clear resin

While clear resin proved to be an ideal choice for fabricating microfluidic channels, SSCCs, or any devices requiring transparency (e. g., for visual observation), there were several challenges related to printing and profilometry that must be taken into consideration. During printing, parts in clear resins were vulnerable to distortion from additional light exposure "bleed" from layers above and below the intended layer. Also, during profilometry, reflection and refraction can distort the

measurements due to changes in the optical properties of the medium.

For channel depths of 0.1–1 mm, the industrial 3-D printed IGS showed a depth difference of $<\!4\%$ between target and measured dimensions (Fig. 2c and d). In contrast, for channel depths of 0.4–1 mm, the consumer-level printer had less than a 6% discrepancy. It exhibited a 12–15% discrepancy for features of 0.1–0.2 mm. The standard deviation of depth measurement ranged from 0.004 to 0.03 mm for the industrial printer. In comparison, the consumer printer had standard deviation values ranging from 0.003 and 0.027 mm.

Analysis of the accuracy of positive features (raised microchannels) of the IGS fabricated with the industrial 3-D printer using clear resins for heights of 0.1–1 mm showed a difference of 0.5–5% between target and measured dimensions (Fig. 2c and d). In contrast, for channel heights of 0.4–1 mm the consumer-level printer had a 15–17% discrepancy. However, this exceeded 33% for channels ranging from 0.1 to 0.2 mm. The standard deviation of height measurements ranged from 0.005 to 0.031 mm for the industrial printer. In comparison, the consumer printer had standard deviation values ranging from 0.017 to 0.063 mm.

For the first five negative stepped features (diameter range from 4.2 mm to 1.8 mm) the depths with the industrial 3-D printer using clear resin had a difference of $<\!4\%$ between target and measured dimensions (Fig. 3b). In contrast, the consumer-level printer had a 2–15% discrepancy in seven stepped-feature depths (diameter range from 4.2 mm to 0.6 mm). Using the settings described herein, the industrial printer failed for the last two bottom (6th and 7th) stepped features with diameters of 1.2 and 0.6 mm. The standard deviation of depth measurements ranged from 0.009 to 0.044 mm for the industrial printer. In comparison, the consumer printer had standard deviation values ranging from 0.07 to 0.039 mm.

For the positive stepped features (diameter range from $4.2 \, \text{mm}$ to $0.6 \, \text{mm}$), accuracy of the industrial 3-D printer showed a difference of <6% between target and measured heights. In contrast, accuracy of positive stepped features produced with the consumer printer was <12% other than the first and second stepped features (diameters of $4.2 \, \text{and} \, 3.6 \, \text{mm}$) which failed to print. The standard deviation of height measurements

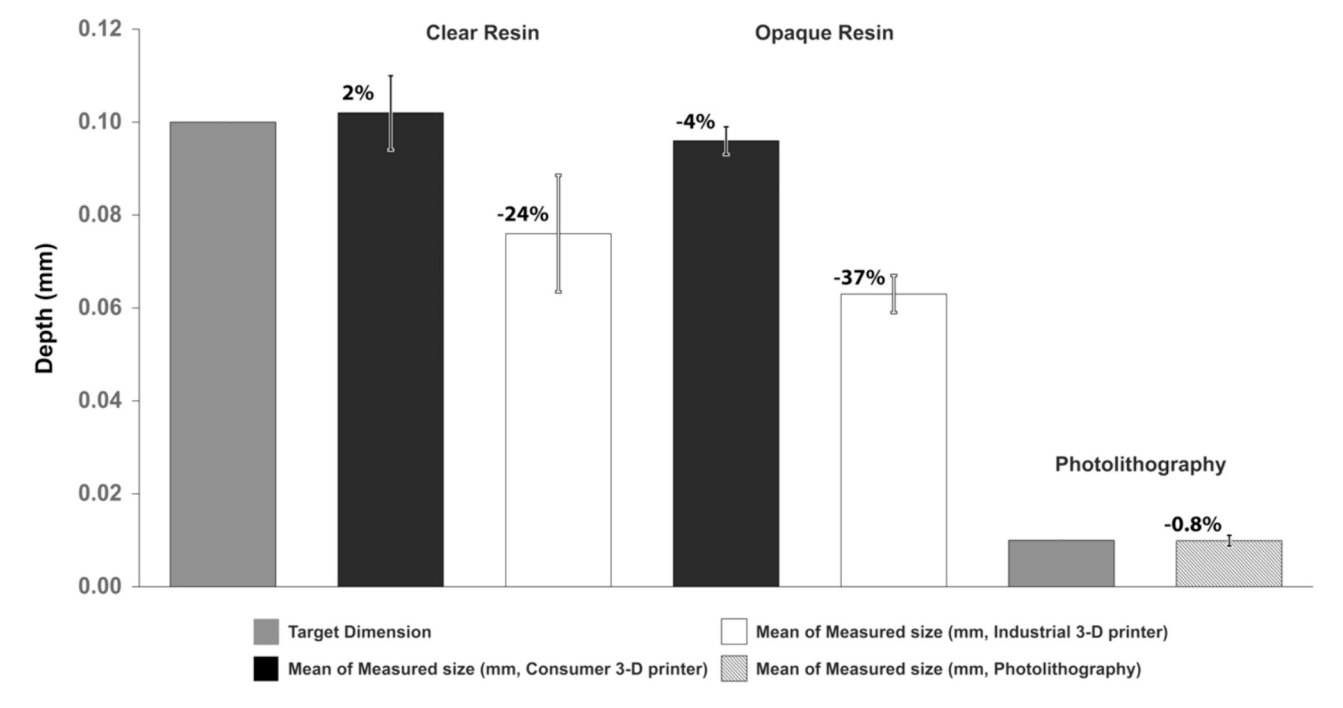


Fig. 4. Comparative analysis of the target depth versus the mean of measured depth using opaque resin and clear resin for SSCC fabricated with an industrial 3-D printer (white), consumer 3-D printer (black), and photolithography (cross-hatched), compared to target dimensions (gray). Percent difference of the mean measured depth from the target depth was indicated at the top of each bar. Standard deviation was indicated by error bars. The target height for SSCC fabricated by use of resin printers was 0.1 mm and the target height for SSCC fabricated by use of photolithography was 0.01 mm. For resin prints, four devices with six measurements per device were averaged. For photolithography, one device with six measurements were averaged.

ranged from 0.01 to 0.022 mm for the industrial printer. In comparison, the consumer printer had standard deviation values ranging from 0.014 to 0.029 mm (Fig. 3b).

Analysis of the accuracy of the clear SSCC (with grid height of 0.1 mm) fabricated with the industrial 3-D printer had a 2% discrepancy between target and measured heights (Fig. 4). The consumer printer had a discrepancy of 24% in dimensional height when utilizing clear resin. The standard deviation for the samples fabricated with the industrial printer was 0.008 mm. Despite the discrepancies for samples fabricated with the consumer printer, the standard deviation was 0.012 mm.

For the photolithography-based SSCC (cast from the wafer), a 0.8% difference between target and measured heights was observed (Fig. 4). The standard deviation was 0.001 mm.

3.3. Visual morphology

Achieving optimal squareness in 3-D printed features posed a notable challenge. Images captured with the optical profilometer illustrated differences in IGS negative features fabricated with industrial and consumer 3-D resin printers using opaque and clear resins (Fig. 5a-e).

In general, deeper features appeared to have better squareness at their bottoms. Visually, the industrial resin printer (Fig. 5a and b) was able to produce sharper angles at the bottom and top of negative features compared with the consumer resin printer (Fig. 5c and d).

Visual analysis of stepped features identified different problems than square features. To facilitate visual analysis, a Keyence tool called "CAD Compare" was used (Fig. 6). The line plots (top of each panel) showed that the industrial printer with opaque resin performed best at depth and height feature fabrication. The consumer printer did well when printing negative features with clear resin, while the industrial printer did better when printing positive features with clear resin. This CAD Compare analysis also assessed the roundness of the cylinders which is important

in some applications but was not directly addressed herein. Visually, the roundness of the cylinders was good with both printer types and resins, until the smallest (deepest and tallest) layers. This was also where the printers struggled to fabricate accurate depths and heights (Fig. 3).

The surface quality of the SSCC imaged by use of scanning electron microscopy (SEM) revealed differences in performance among the fabrication methods (Fig. 7a-c). This showed the pre-selected difference in grid-wall height between the photolithography-based (0.01 mm) and resin-based (0.1 mm) SSCCs. The channels between grids were reliably fabricated with photolithography and the surface detail at the bottom of each cell was smooth (Fig. 7a). In resin-based devices, the channels between the grids were not reliably created, although the surface detail was relatively smooth (Fig. 7b and c). A texturing is visible resembling the pixel pattern from the printer LCD. Of note are the visible layer lines produced with the industrial 3-D resin printer (Fig. 7b). The grid walls appear to be 2-layer lines thick (0.03 mm layer height and 0.1 mm target grid height).

To evaluate post-processing, SEM images of SSCC were captured before and after removal of residual resin (Fig. 8a and b). One interesting observation was that post-processing revealed the channels between the grids, which were important for even filling and cellular distribution within the device.

In the final phase of post-processing, UV exposure was applied to the samples for 1 min, enhancing mechanical properties but sometimes introducing a curvature [35]. Various printing parameters including print time, single-layer height, post-curing UV intensity, and total thickness have been reported to play substantial roles in this curvature phenomenon [36]. Images of SSCC with and without post-processing (UV exposure) were captured with the profiler (Fig. 9a and b). Curling was evident in the UV-exposed sample. To mitigate this, an approach was developed allowing the sample to remain affixed to the build plate for approximately 24 h after UV exposure (data not shown). This served

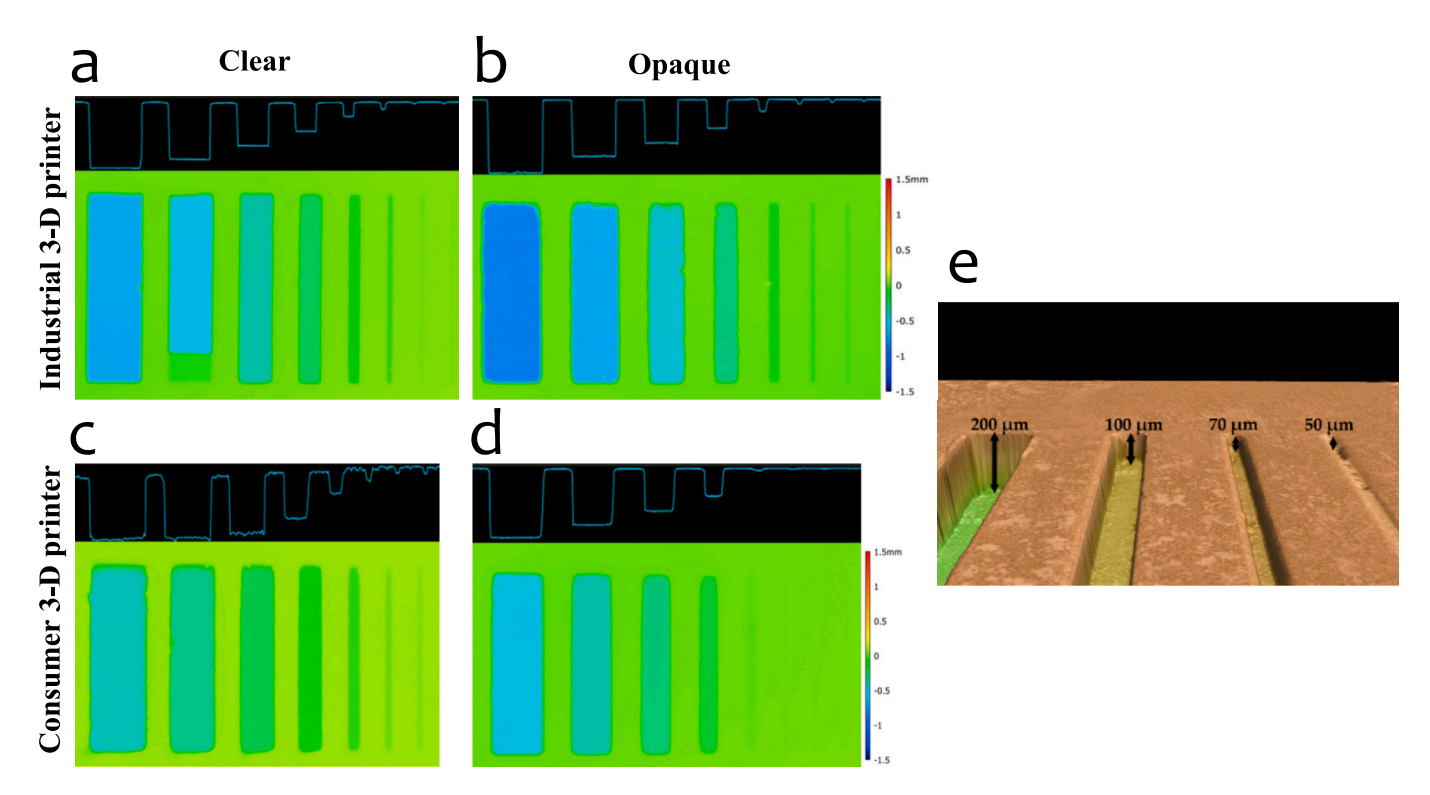


Fig. 5. Two-dimensional images produced by optical profiling of IGS channels with square cross-sectional design (ranging from 1 mm to 0.05 mm) fabricated with industrial 3-D printer using clear resin (panel a), industrial 3-D printer using opaque resin (b), consumer printer using clear resin (c), consumer printer using opaque resin (d), in comparison to a representative 3-D image (industrial printer using opaque resin) of the negative features (e). Blue colors indicate values below the reference plane and green colors indicate depths closer or equal to the reference plane. (For interpretation of the references to colour in this figure legend, the reader is referred to the web version of this article.)

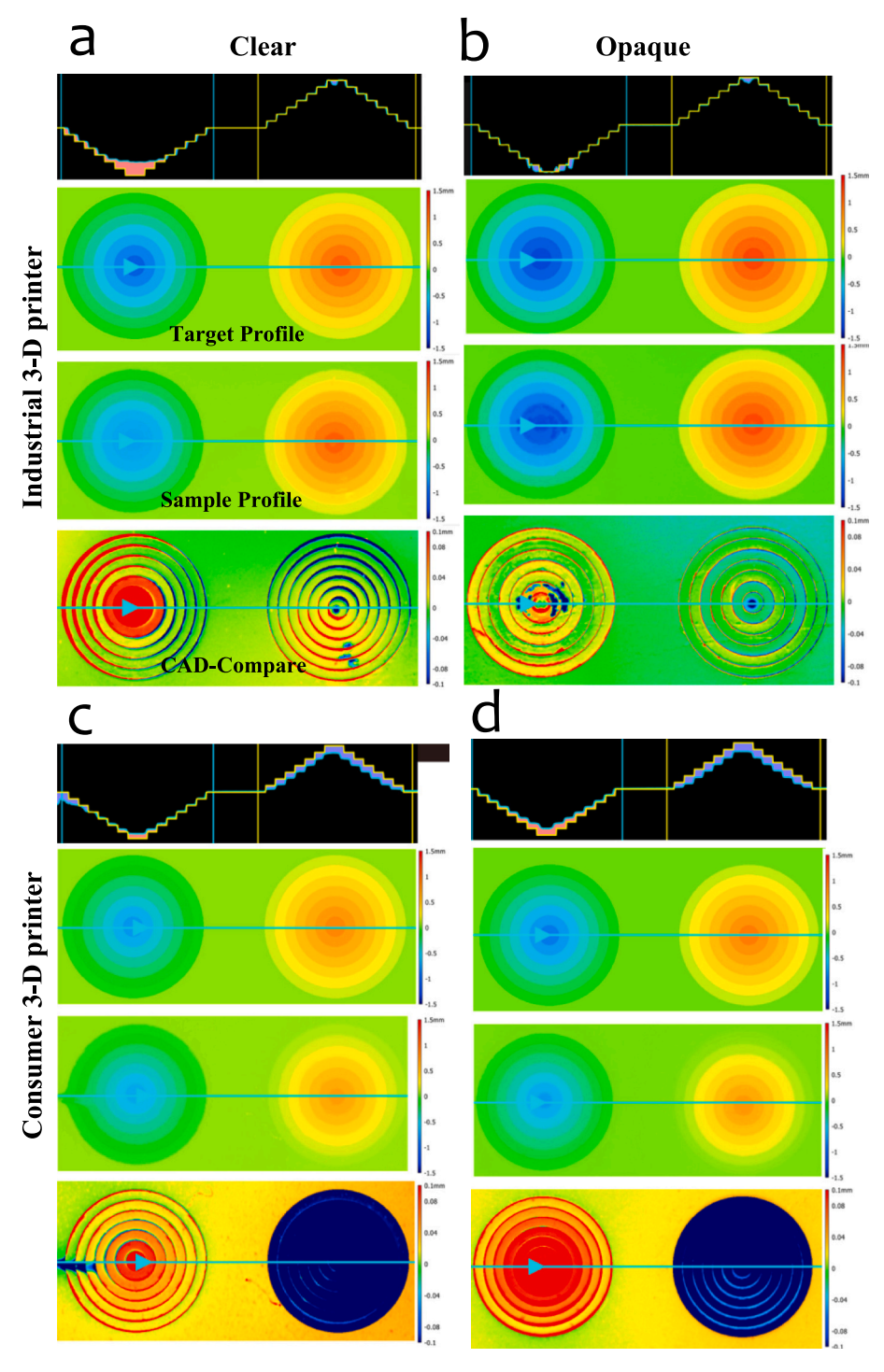


Fig. 6. Images produced by optical profiling of IGS stepped features for target profile, sample profile, and CAD comparison (height difference between target and printed sample) for the industrial 3-D printer with clear resin (panel a), industrial 3-D printer with opaque resin (b), consumer printer with clear resin (c) and, consumer printer with opaque resin (d). Reds indicated measured depths that were shallower than the target, green indicated measured depths and heights that were near or equal to the target, and blues indicated measured heights that were shorter than the target. (For interpretation of the references to colour in this figure legend, the reader is referred to the web version of this article.)

as an effective method to alleviate stress in the printed samples, contributing to the reduction of curvature induced by post-processing.

3.4. Comparison of time and cost of microfabrication

Efficiency and cost-effectiveness are pivotal factors in selecting microfabrication techniques for creation of microdevices [31]. In terms of fabrication time, fabrication of a single SSCC with photolithography

typically required around 2 d and cost US\$555 (Table 1). However, utilizing industrial and consumer-grade 3-D resin printers significantly reduced time and material costs. For example, the industrial printer fabrication time was <38 min and cost as little as US\$0.08 per unit (Table 1). The cost calculations (Supplementary Table 2) did not include salary, electrical, or other facilities and personnel costs because these vary by location. The time calculations did not take into consideration the new approach to mitigate post-UV exposure curvature because it

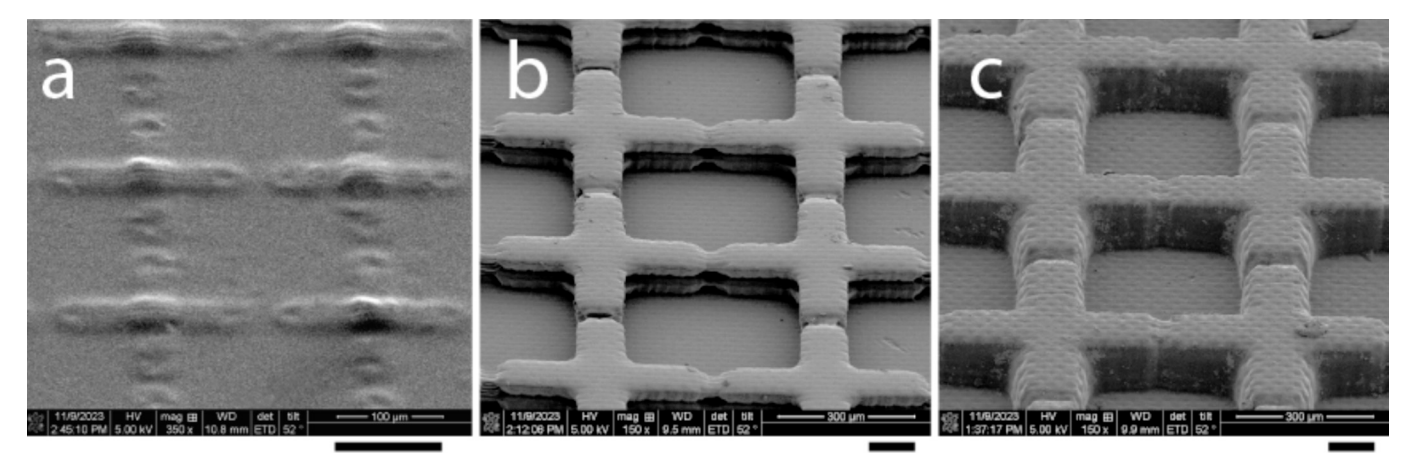


Fig. 7. Scanning electron microscopy of SSCC devices fabricated using: photolithography (panel a), industrial 3-D resin printing (b), and consumer 3-D printing (c) (scale bars = 0.1 mm). The SSCC consisted of grid and wall features with heights of 0.01 mm (photolithography) or 0.1 mm (resin printing), including gaps in the gridlines that connected the squares to allow better distribution of sample for counting or quality evaluation (e.g., sperm motility) of biological samples.

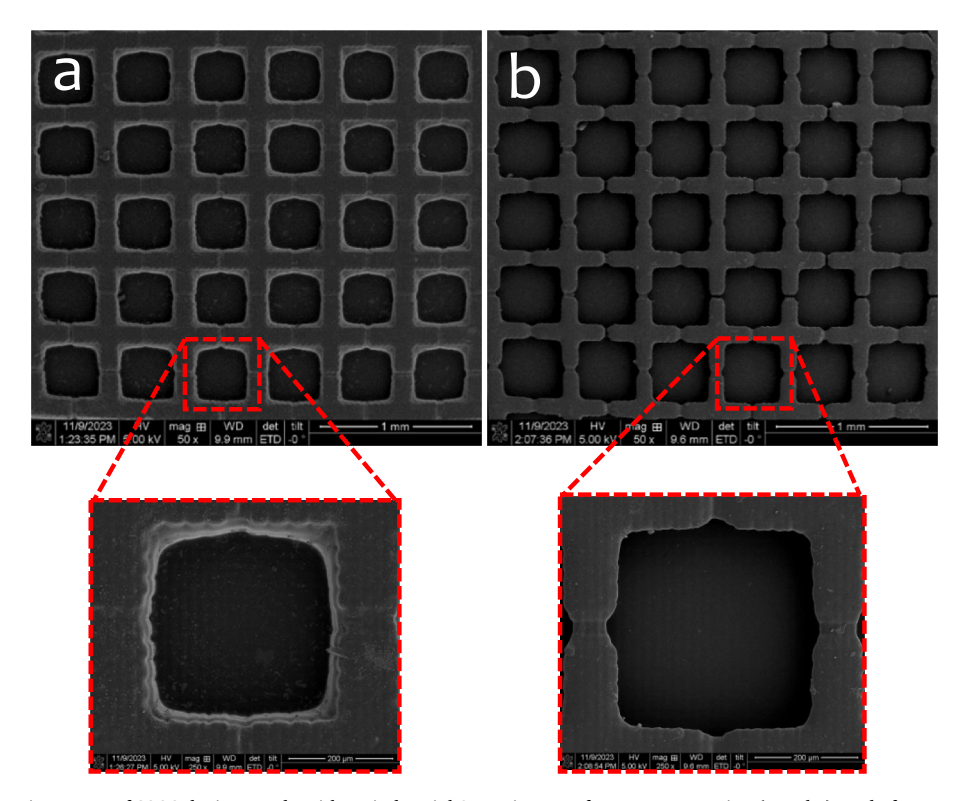


Fig. 8. Scanning electron microscopy of SSCC devices made with an industrial 3-D printer. Before post-processing (panel a), and after post-processing (b) (removing residual resin with IPA).

may not be necessary for all device configurations.

4. Discussion

This study evaluated dimensional accuracy and precision, visual morphology, and squareness of depth and height features in devices fabricated by use of traditional photolithography and industrial and consumer-grade 3-D resin printers using opaque and clear resin. In addition, the time and cost requirements were evaluated for microfabrication among the methods. The findings of this study underscored the comprehensive capabilities of industrial-grade and consumer-grade 3-D printers, in relation to photolithography in meeting complex dimensional requirements for specific applications. For this evaluation, the SSCC provided a device with direct relevance to biological usage,

and the IGS allowed evaluation of fabrication quality of 3-D resin printers across a range of features. In the selection of IGS features, square geometries were chosen due to their prevalence and significance in microfluidic applications which were the primary focus of this study. Depth and height of stepped features also hold significance in certain applications and pose challenges during fabrication and were thus also chosen for evaluation. Dimensional accuracy and precision and squareness of depth and height features are critical factors for the use of quality management devices for germplasm. Differences in fabrication quality translate to functional performance changes, affecting accuracy of metrics such as sperm concentration which requires accurate volumetric calculations or microfluidic mixing efficiency needing precise feature angles and placement.

The industrial 3-D printer consistently exhibited close accuracy and

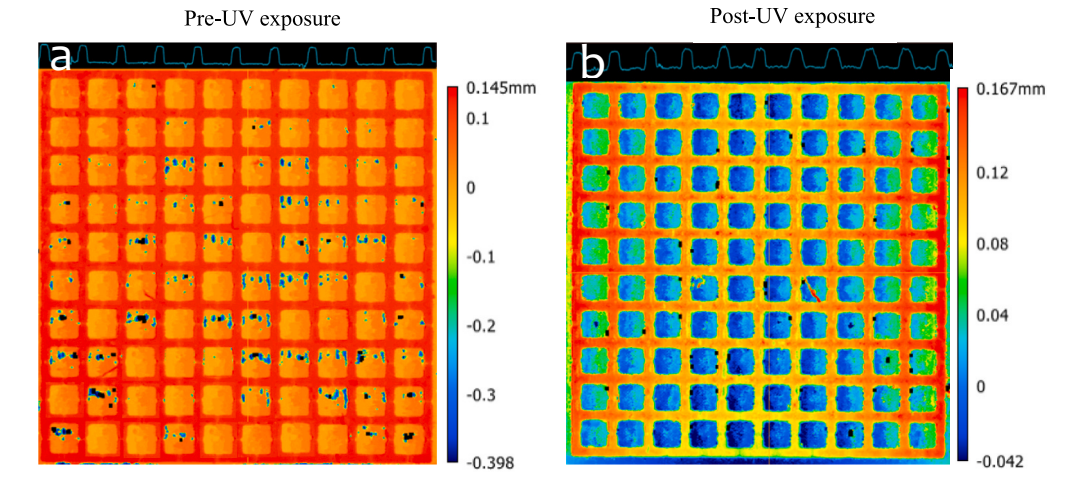


Fig. 9. Profiled height of a SSCC device produced by the industrial printer, before curing (panel a), and after curing demonstrating curling (b) (UV exposure). The colour indicates the depth relative to a baseline of zero. Note the difference in scales. Orange indicates measurements equal to the reference plane (a). Reds indicate measurements above, the reference plane and greens and blues indicate measurements below the reference plane (a). Blue indicates measurements equal to the reference plane (b). Reds, oranges, and greens indicate measurements above the reference plane (upward curvature) (b). (For interpretation of the references to colour in this figure legend, the reader is referred to the web version of this article.)

Table 1
Fabrication time and cost (per unit) for industrial and consumer 3-D resin printed IGS and industrial, consumer 3-D resin printed and photolithography-based SSCC.
Cost calculations are rounded to the nearest cent.

Fabrication Method	Time (min)				Unit Cost (US\$)			
	IGS		SSCC		IGS		SSCC	
	Clear	Opaque	Clear	Opaque	Clear	Opaque	Clear	Opaque
Photolithography	_	_	~960	_	-	-	~555	_
Industrial resin	22	22	9	9	~0.32	~0.28	~0.08	~0.07
Consumer resin	128	88	48	38	~0.03	~0.03	~0.01	~0.01

precision aligned with the photolithography-based SSCC for microchannel fabrication using clear resin, even with minimum feature sizes as small as 0.1 mm. Conversely, the consumer 3-D printer, although less accurate and precise for features smaller than 0.2 mm, demonstrated reliability for features above this threshold. The larger variations, especially for raised features, were likely attributable to the specific printer settings. Throughout preliminary preparation for this study, numerous settings were explored to establish a balance for the evaluation of positive and negative features in the same device. The settings outlined in Supplementary Table 1 were identified as being effective for the specific purposes of this study.

As with traditional fabrication approaches, 3-D printing has a tradeoff between extensive optimization for accuracy and precision, and the
need for rapid prototyping or production of parts that do not require
high tolerances [37]. With targeted refinements it would be possible to
identify specific print settings for the consumer-grade printer that would
further enhance the quality of the positive or negative features, but this
was not the intent of the study. Industrial printers require less adjustment of such settings as they are already optimized for specific applications (e.g., microfabrication in the present study). In fabricating
opaque SSCCs using consumer-grade printers, we encountered instances
where the devices exhibited high precision comparable to the industrialgrade printer but lacked in accuracy (Fig. 4). Through experimentation
involving iterative prototyping and adjustments to factors such as resin
types and print settings, achieving a practical balance between accuracy
and precision appeared to be achievable.

Stepped features printed with an industrial printer, had positive features (using opaque and clear resins) within 6% of the target dimensions, and thus exhibited reliable accuracy. However, the 6th (1.2 mm diameter) and 7th (0.6 mm diameter) negative stepped features

failed to print reliably. This could be attributed to several factors including the round shape of features with small diameters, or the print settings, which may pose challenges for printing. Surprisingly, this was less challenging with the consumer printer. Instead, the consumer printer had problems with the 1st (4.2 mm diameter) and 2nd (3.6 mm diameter) positive stepped features using opaque and clear resins. Due to the higher sensitivity of consumer machines to print settings, achieving better results may be possible through adjustments to these settings. Future evaluations of the roundness (X-Y orientation) of round features on the IGS will provide insight into the potential limitations of LCD-based resin 3-D printers to fabricate round features.

These results highlighted the capabilities of different fabrication methods in terms of accuracy and precision across different feature sizes and types. It established industrial 3-D resin printers as a strong option for applications requiring high-resolution microfabrication, while consumer printers remain a viable choice for less demanding applications where feature sizes are not as critical or where there is more time for optimization of settings and resin types. The rapid advancements being made in consumer 3-D resin printing open substantial opportunities for achieving reliable microfabrication in the future. With respect to aquatic organisms, even the consumer-level printers provided sufficient accuracy and precision for routine practical use with most species and germplasm types.

The width resolution (not directly examined herein), is intricately linked to the X-Y resolution and is influenced by the size of the projected pixels. It operates in conjunction with depth resolution, which is closely tied to Z resolution, representing the thickness of each cured layer [38]. These interrelated factors collectively contributed to the overall accuracy, precision, and level of detail attainable in printed objects. In exploring the relationship between printing orientation and dimensional

accuracy and precision, altering printing orientation by 90 degrees could potentially result in a reduction in the variance of depth dimensions compared to width [39,40]. Changing the print orientation may thus influence the dimensional accuracy and precision of features within devices like the SSCC. These considerations should be investigated further and offer another avenue for reducing differences and variations observed in the depth dimensions from the printers.

In terms of visual squareness, the industrial 3-D resin printer using clear resin produced sharper corners in channels compared to prints with opaque resin (Fig. 5). When assessing the final output, it was essential to consider the influence of the slicer settings on dimensions and printer resolution. The industrial printer produced channels of ≥ 0.1 mm with minimal defects. However, potential defects, particularly in the roundness of the edges, become noticeable for channels smaller than 0.1 mm, affecting positive and negative features under these conditions. The consumer 3-D resin printer using opaque resin produced sharper corners in channels compared to prints with clear resin but was able to produce smaller channels better with the clear resins (Fig. 5). These visual observations of squareness between the two printer types demonstrates the opportunities to advance their capabilities and could be helpful in deciding which printer type would be best suited for specific applications that require square-angle features in clear or opaque.

Surface morphology plays a crucial role in determining the functionality and performance of microdevices. For instance, in biomedical devices it can affect cell adhesion and proliferation [41]. The industrial 3-D printer produced visually smoother surfaces compared to prints with the consumer 3-D printer (Fig. 7b and c). This superior surface quality could contribute to enhanced functionality and reliability of microfluidic channels fabricated using industrial-grade 3-D printing, highlighting its potential for various applications requiring high-quality surface finishes. Comparatively, the photolithography-based SSCC exhibited a visually smoother surface (Fig. 7a) with fewer defects than devices created by the industrial 3-D resin printer. The effect of these differences in surface morphology on the functionality and performance of resin-printed devices requires further investigation and will vary across the range of devices and functionalities desired.

For stepped features, squareness and roundness of the edges were significant factors. These parameters appeared to be satisfactory for industrial 3D-printed samples. However, in the case of consumer 3D-printed samples, while the roundness appeared acceptable, there were noticeable issues with edge squareness. The CAD comparisons showed differences in depth or height of negative or positive features compared to the design. The industrial and consumer printers generally produced better surface morphology for positive stepped features compared to negative features.

The photolithography-based method, despite its time-intensive 2day fabrication process and substantial cost of approximately US\$555 per unit for SSCC fabrication, distinguished itself through accuracy, precision, and control. This makes it particularly well-suited for applications that prioritize exacting accuracy and precision, such as highly quantitative analysis of the smallest of aquatic germplasm types (e.g., zebrafish sperm). It should be noted that the unit cost associated with photolithography decreases once a finalized mold is generated because many devices can be cast from one mold [15]. Although, the unit cost could also increase drastically if customization or changes need to be made to a mold which would require repeating the mold creation process. Industrial resin 3-D printing was efficient, requiring <30 min for IGS and SSCC fabrication with material costs estimated at US\$0.32 per unit for clear IGS and US\$0.08 for clear SSCC. This method enhanced rapid prototyping and fabrication. On the other hand, consumer resin 3-D printing struck a balance between fabrication time and cost, providing relatively fast times (<150 min) for IGS and SSCC (clear and opaque), with costs estimated at US\$0.03 per unit for clear IGS and US\$0.01 for clear SSCC. This presents a cost-effective solution for open-hardware applications with budgetary constraints while providing satisfactory fabrication times across the size and resolution range needed for aquatic

species. Overall, photolithography can provide accuracy and precision, industrial resin 3-D printing can be useful for rapid prototyping, and consumer resin 3-D printing offers a balance between efficiency and cost-effectiveness, with these differences operating along a gradient of scale.

Aquatic species are in great need for powerful and innovative solutions requiring rapid prototyping and, at a minimum, batch fabrication. Currently, the resolution for resin printing is sufficient for these applications, and eventually printers that can compete directly with soft lithography will become cheap enough to be accessible to the broader community. Moving forward, devices created by use of 3-D resin printing will require testing to ensure accuracy and functionality, and resins will need to be evaluated for cytotoxicity. Though it is important to note that resin contact with sperm is for a short duration (1-2 s) and devices can make use of a disposable sub-sample rather than the entire sample. Even with the current capabilities of resin printing, we can move seamlessly from micro- to milli- to macro- scales in the design process without changing materials or equipment. Overall, the dynamic range of resin printing demonstrated herein enables high precision and throughput that can extend into open hardware, promoting inclusive access to critical technology and fostering community-driven innovation for aquatic species.

In addition, all the architecture necessary for a single device (e.g., Luer locks and other connections) can be printed at one time and in one material enabling direct single-step production of devices. However, resin printers are not limited to direct production and, like photolithography, can also print device molds facilitating access, distribution, and community development. By adding 3-D resin printing to the roster, designers, fabricators, and users now have multiple options for developing and obtaining devices. The greatly broadened accessibility of resin 3-D printers compared to photolithography provides new opportunities for standardized designs and procedures. This approach empowers wider dissemination and adoption within research and aquaculture communities, accelerating the transition to open hardware and sustainable germplasm repository development. By cultivating an international community capable of independent fabrication and design, a collaborative system can emerge to enhance genetic resource protection and promote much-needed innovation in culture, breeding, conservation, and research of aquatic species.

5. Conclusions

This study provided an overall evaluation of the capabilities of representative industrial-grade and consumer-level 3-D resin printing compared to conventional photolithography in fabrication of microdevices with a specific focus on germplasm repository development for aquatic species. This provides a platform for improving critical QM strategies throughout genetic resource protection processes. Fabrication quality distinctions were highlighted through the assessment of various components in microdevices including positive and negative features, channels, and complex structures. Visual morphologic analysis revealed differences in squareness and roundness, emphasizing the importance of considering these factors in the design of devices and the selection of fabrication technologies.

Overall, this research contributes to the ongoing exploration of emerging technologies in microdevice development and prototyping. By understanding the strengths and limitations of 3-D resin printing technologies, researchers and industry professionals can make informed decisions when selecting fabrication methods for specific applications. As the field progresses, studies of this type can provide a solid foundation for future advancements in custom microdevice creation, particularly with essential germplasm repository technology for aquatic species. By pioneering a shift from traditional methods to 3-D resin printing, the stage can be set for more efficient and precise fabrication processes. In addition, insights into the trade-offs between consumergrade and industrial-grade printers can guide technology selection

facilitating broader accessibility and innovation. Such findings will fuel development of standardized protocols, open-hardware designs, and novel solutions, ultimately enhancing aquatic species conservation efforts and genetic resource preservation. Interdisciplinary approaches such as these integrating biology and engineering (e.g., [42]) in a real-world context offer powerful mechanisms for producing innovation to address future challenges including climate change.

Declaration of competing interest

The authors declare that they have no known competing financial interest or personal relationships that could have appeared to influence the work reported in this paper.

Data availability

Summarized data are available at the AGGRC github: $\frac{\text{https://github.com/aggrc/resin-PDMS}}{\text{com/aggrc/resin-PDMS}}$

Acknowledgments

This work was supported in part by the Louisiana State University Agricultural Center Agriculture Collaborative Research Program Grant, with additional support provided by the National Institutes of Health (NIH) Office of Research Infrastructure Programs (ORIP) (R24-OD034058 to Jose Cibelli and R24-OD028443), the National Institute of Food and Agriculture, United States Department of Agriculture (Hatch project LAB94643), the National Science Foundation (Award 2229680), and Louisiana State University Agricultural Center Program for Enhancement of External Competitive Funding. We thank C. Bonds, J. Dugas, and J. Belgodere for technical assistance. This manuscript was approved for publication by the Louisiana State University Agricultural Center as number 2024-241-39745.

Appendix A. Supplementary data

Supplementary data to this article can be found online at https://doi.org/10.1016/j.mne.2024.100277.

References

- [1] N. Coxe, Y. Liu, L. Arregui, R. Upton, S. Bodenstein, S.R. Voss, M.T. Gutierrez-Wing, T.R. Tiersch, Establishment of a practical sperm cryopreservation pathway for the axolotl (*Ambystoma mexicanum*): a community-level approach to germplasm repository development, Animals (Basel) 14 (2024) 206.
- [2] I. Haagen, H. Blackburn, Efforts to cryopreserve shrimp (Penaeid) genetic resources and the potential for a shrimp germplasm bank in the United States, Aquaculture 580 (2023) 740298.
- [3] J.C. Koch, A.M. Oune, S. Bodenstein, T.R. Tiersch, Untangling the Gordian Knot of Aplysia sea hare egg masses: an integrated open-hardware system for standardized egg strand sizing and packaging for cryopreservation research and application, HardwareX 16 (2023) e00476.
- [4] Y. Liu, J.C. Koch, L. Arregui, A. Oune, S. Bodenstein, M.T. Gutierrez-Wing, T. R. Tiersch, Exploring pathways toward open-hardware ecosystems to safeguard genetic resources for biomedical research communities using aquatic model species, J. Exp. Zool. B Mol. Dev. Evol. (2024) 278–290.
- [5] R.S.V. Pullin, Genetic resources for aquaculture: Status and trends, in: Status and Trends in Aquatic Genetic Resources: A Basis for International Policy, 2006.
- [6] T.R. Tiersch, C.C. Green, Cryopreservation in Aquatic Species: A Comprehensive Overview of Current Practices, Programmatic Development and Future Directions for Cryopreservation of Gametes Embryos and Larvae of Aquatic Species, World Aquaculture Society, 2011.
- [7] Y. Liu, W.T. Monroe, J.A. Belgodere, J.-W. Choi, M.T. Gutierrez-Wing, T.R. Tiersch, The emerging role of open technologies for community-based improvement of cryopreservation and quality management for repository development in aquatic species, Anim. Reprod. Sci. 246 (2022) 106871.
- [8] M.R.I. Sarder, Potential of Fish Gamete Cryopreservation in Conservation Programs in Bangladesh, in: Cryopreservation of Fish Gametes, Springer Singapore, Singapore, 2020, pp. 337–344.
- [9] S. Bodenstein, T.R. Tiersch, M.A.R. Hossain, M.G. Hamilton, M. Yeasin, M. M. Akhter, T.Q. Trinh, M. Mahmuddin, A cryopreserved sperm repository strategy for WorldFish genetically improved carp, 2023.

- [10] W. Wang, J. Zhang, C. Xu, Oscillating feedback micromixer: a short review, Chemical Engineering and Processing-Process Intensification 109812 (2024).
- [11] R. Ghosh, A. Arnheim, M. van Zee, L. Shang, C. Soemardy, R.-C. Tang, M. Mellody, S. Baghdasarian, E. Sanchez Ochoa, S. Ye, Lab on a particle technologies, Anal. Chem. 96 (2024) 7817–7839.
- [12] A. Ebrahimi, K. Icoz, R. Didarian, C. Shih, E.A. Tarim, B. Nasseri, A. Akpek, B. Cecen, A. Bal-Ozturk, K. Güleç, Molecular separation by using active and passive microfluidic chip designs: a comprehensive review, Adv. Mater. Interfaces 11 (2024) 2300492.
- [13] M. Hagedorn, Z. Varga, R.B. Walter, T.R. Tiersch, Workshop report: cryopreservation of aquatic biomedical models, Cryobiology 86 (2019) 120–129.
- [14] Y. Liu, M. Chesnut, A. Guitreau, J. Beckham, A. Melvin, J. Eades, T.R. Tiersch, W. T. Monroe, Microfabrication of low-cost customisable counting chambers for standardised estimation of sperm concentration, Reprod. Fertil. Dev. 32 (2020) 873–878.
- [15] J.A. Belgodere, Y. Liu, E.L. Reich, J. Eades, T.R. Tiersch, W.T. Monroe, Development of a single-piece sperm counting chamber (SSCC) for aquatic species, G 7 (2022) 231.
- [16] J. Beckham, F. Alam, V. Omojola, T. Scherr, A. Guitreau, A. Melvin, D.S. Park, J.-W. Choi, T.R. Tiersch, W. Todd Monroe, A microfluidic device for motility and osmolality analysis of zebrafish sperm, Biomed. Microdevices 20 (2018) 67.
- [17] D.S. Park, R.A. Egnatchik, H. Bordelon, T.R. Tiersch, W.T. Monroe, Microfluidic mixing for sperm activation and motility analysis of pearl *Danio* zebrafish, Theriogenology 78 (2012) 334–344.
- [18] D.S. Park, C. Quitadamo, T.R. Tiersch, W.T. Monroe, Microfluidic mixers for standardization of computer-assisted sperm analysis, Cryopreservation in Aquatic Species 2 (2011) 261–272.
- [19] S. Razavi Bazaz, N. Kashaninejad, S. Azadi, K. Patel, M. Asadnia, D. Jin, M. Ebrahimi Warkiani, Rapid softlithography using 3D-printed molds, Advanced Materials Technologies 4 (2019) 1900425.
- [20] R. Rahul, N. Prasad, R.R. Ajith, P. Sajeesh, R.S. Mini, R.S. Kumar, A mould-free soft-lithography approach for rapid, low-cost and bulk fabrication of microfluidic chips using photopolymer sheets, Microfluid. Nanofluid. 27 (2023) 78.
- [21] C. He, S. Li, B. Jiang, F. Chen, W. Hu, F. Deng, Surface hydrophobicity and guest permeability in polydimethylsiloxane-coated MIL-53 as studied by solid-state nuclear magnetic resonance spectroscopy, ACS Appl. Mater. Interfaces 15 (2023) 37936–37945.
- [22] J. Lee, J. Kim, H. Kim, Y.M. Bae, K.-H. Lee, H.J. Cho, Effect of thermal treatment on the chemical resistance of polydimethylsiloxane for microfluidic devices, J. Micromech. Microeng. 23 (2013) 035007.
- [23] A.E. Lenhart, R.T. Kennedy, Evaluation of surface treatments of PDMS microfluidic devices for improving small-molecule recovery with application to monitoring metabolites secreted from islets of Langerhans, ACS Measurement Science Au 3 (2023) 380–389.
- [24] A. Mata, A.J. Fleischman, S. Roy, Characterization of polydimethylsiloxane (PDMS) properties for biomedical micro/nanosystems, Biomed. Microdevices 7 (2005) 281–293.
- [25] A.-G. Niculescu, C. Chircov, A.C. Bîrcă, A.M. Grumezescu, Fabrication and applications of microfluidic devices: a review, Int. J. Mol. Sci. 22 (2021), https:// doi.org/10.3390/ijms22042011.
- [26] M.W. Toepke, D.J. Beebe, PDMS absorption of small molecules and consequences in microfluidic applications, Lab Chip 6 (2006) 1484–1486.
- [27] W.M. Childress, Y. Liu, T.R. Tiersch, Design, alpha testing, and beta testing of a 3-D printed open-hardware portable cryopreservation device for aquatic species, J. Appl. Aquac. 35 (2023) 213–236.
- [28] Y. Liu, M. Eskridge, A. Guitreau, J. Beckham, M. Chesnut, L. Torres, T.R. Tiersch, W.T. Monroe, Development of an open hardware 3-D printed conveyor device for continuous cryopreservation of non-batched samples, Aquac. Eng. 95 (2021) 102202.
- [29] A. Amini, R.M. Guijt, T. Themelis, J. De Vos, S. Eeltink, Recent developments in digital light processing 3D-printing techniques for microfluidic analytical devices, J. Chromatogr. A 463842 (2023).
- [30] M.J. Schwing, Y. Liu, J.A. Belgodere, W.T. Monroe, T.R. Tiersch, A. Abdelmoneim, Initial assessment of the toxicologic effects of leachates from 3-dimensional (3-D) printed objects on sperm quality in two model fish species, Aquat. Toxicol. 256 (2023) 106400.
- [31] N.C. Zuchowicz, J.A. Belgodere, Y. Liu, I. Semmes, W.T. Monroe, T.R. Tiersch, Low-cost resin 3-D printing for rapid prototyping of microdevices: opportunities for supporting aquatic germplasm repositories, G 7 (2022), https://doi.org/10.3390/ fishes7010049.
- [32] R. Zhou, M. Versace, B. Boisnard, M. Gómez-Castaño, C. Viana, J.-L. Polleux, A.-L. Billabert, Thermal stability of SU-8 low-loss optical coupling interconnects at 850 nm, IEEE Photon. Technol. Lett. 36 (2023) 159–162.
- [33] D. Qin, Y. Xia, G. Whitesides, Soft lithography for micro- and nanoscale patterning, Nat. Protoc. 5 (2010) 491–502.
- [34] S.M. Montgomery, F. Demoly, K. Zhou, H.J. Qi, Pixel-level grayscale manipulation to improve accuracy in digital light processing 3D printing, Adv. Funct. Mater. 2213252 (2023).
- [35] S. Aati, Z. Akram, B. Shrestha, J. Patel, B. Shih, K. Shearston, H. Ngo, A. Fawzy, Effect of post-curing light exposure time on the physico-mechanical properties and cytotoxicity of 3D-printed denture base material, Dent. Mater. 38 (2022) 57–67.
- [36] D. Wu, Z. Zhao, Q. Zhang, H.J. Qi, D. Fang, Mechanics of shape distortion of DLP 3D printed structures during UV post-curing, Soft Matter 15 (2019) 6151–6159.
- [37] A.R. Renner, E. Winer, Exploring print setting tradeoffs to improve part quality using a visual thermal process simulation, Adv. Eng. Softw. 173 (2022) 103243.

- [38] B.N. Dhanunjayarao, N.V.S. Naidu, Assessment of dimensional accuracy of 3D printed part using resin 3D printing technique, Materials Today: Proceedings 59 (2022) 1608–1614.
- [39] S. Martínez-Pellitero, M.A. Castro, A.I. Fernández-Abia, S. González, E. Cuesta, Analysis of influence factors on part quality in micro-SLA technology, Procedia Manuf. 13 (2017) 856–863.
- [40] J.S. Shim, J.-E. Kim, S.H. Jeong, Y.J. Choi, J.J. Ryu, Printing accuracy, mechanical properties, surface characteristics, and microbial adhesion of 3D-printed resins with various printing orientations, J. Prosthet. Dent. 124 (2020) 468–475.
- [41] H.-Y. Chang, W.-L. Kao, Y.-W. You, Y.-H. Chu, K.-J. Chu, P.-J. Chen, C.-Y. Wu, Y.-H. Lee, J.-J. Shyue, Effect of surface potential on epithelial cell adhesion, proliferation and morphology, Colloids Surf. B Biointerfaces 141 (2016) 179–186.
- [42] C.A. Graham, H. Shamkhalichenar, V.E. Browning, V.J. Byrd, Y. Liu, M. T. Gutierrez-Wing, N. Novelo, J.-W. Choi, T.R. Tierschc, A practical evaluation of machine learning for classification of ultrasound images of ovarian development in channel catfish (*Ictalurus punctatus*), Aquaculture 552 (2022), https://doi.org/10.1016/j.aquaculture.2022.738039.